Axial Flow Marine Turbine Rotor Spacing Influence on Power Performance: Simulating a 1:40 Scale Dual-Rotor Counter-Rotating Turbine (US DOE RM1)

Javier Guzmán[1], Craig Hill[1,2]

1. University of Minnesota Duluth, Mechanical and Industrial Engineering Department
2. Institute on the Environment, University of Minnesota

Keywords— **Axial flow marine turbine, computational fluid dynamics, sliding mesh technique, turbine power estimation, wake modeling**

I. Introduction

Due to the rise in global energy demand, fossil fuel use and demand results in higher carbon emissions [1]. This high dependency on fossil fuels could be alleviated with renewable energy sources, such as solar, wind, biomass, geothermal, oceanic, and hydropower, which provide more sustainable and extractable energy [2, 3]. Among them, marine renewable energy (MRE) is a promising option for regions with areas access to MRE resources [4]. The Powering the Blue Economy (PBE) project aims to use MRE to support coastal and maritime markets and promote sustainable development. In the United States, MRE could supply 57% of its 2019 energy demand from marine sources using current technology, according to an estimate that only considers high-generation areas [5]. However, the technologies to extract this type of energy are still in the growth stage, requiring significant research and development to make them competitive with other technologies on a commercial scale. The Reference Model (RM) project was a US Department of Energy (DOE) initiative to advance MRE technologies and stimulate academic and industry research using six open-source reference models (RM1 to RM6) for extracting energy from currents and waves, based on real sites in the US.

With rapidly developing computational resources, researchers are making use of powerful computational fluid dynamics (CFD) simulations to analyze various phenomena that modify the extracted power and characterize the wake of MRE devices. Channel blockage effects on the power extracted by axial and cross-flow MRE turbines have also been investigated using CFD, finding that higher blockage leads to superior power extracted. It was also found that the flow recovers faster with higher blockage, due to enhanced energy transfer between varying wake velocity zones [6, 7]. Other parameters such as drag ratio, power, and Tip Speed Ratio (TSR) of unconfined turbines have been explored, including the differences from confined turbines [8]. Also, CFD has been used across a broad range of MRE technology studies, including wake recovery and interactions, impacts of free surface proximity, and power extraction across a range of TSR [9, 10, 11].

Few numerical studies have been carried out on the RM1 tidal turbine to fully characterize the wake and analyze geometric modifications that could enhance power production and wake recovery. Javaherchi et al. compared the Rotating Reference Frame (RRF) and Blade Element Method (BEM) models and found their limitations for different TSR ranges [12, 13]. Niebuhr et al. validated their numerical model with experimental data in [14], and evaluated various turbulence models, boundary conditions, and rotor modeling techniques using Siemens STAR-CCM+ [15]. In this study, the turbine analyzed consisted of a scaled model of the DOE RM1 turbine, a dual-rotor axial flow marine turbine with counter-rotating rotors, each with a diameter of $d_T = 0.5$ m. The simulations were carried out using the unsteady Reynolds Averaged Navier Stokes (URANS) Shear Stress Transport (SST) $k-\omega$ turbulence model and the sliding mesh technique. Numerical results of turbine performance and wake evolution were compared and validated against experimental [14] and numerical data [15]. Finally, three lateral spacings between rotors' centerlines were studied to evaluate the relationship between this spacing and the overall power production.

II. Geometrical configuration and simulation set-up

A. Numerical domain

The turbine considered in the present study is a 1:40 scale model of the US DOE RM1. This turbine is an axial-flow dual counter-rotating rotors, each with a rotor diameter of $d_T = 0.5$ m. Each rotor and nacelle is mounted on a crossarm assembly which is fixed on a monopile foundation and a $1.4d_T$ lateral distance between the rotors' centers exists. The whole assembly was placed in an open-channel domain that extended -8 d_T upstream to 30 d_T downstream of the axis of rotation. This inlet domain length was selected to allow full flow development before the rotor was reached and it is particular to each case studied as it depends on multiple factors such as the

turbulence model used, TSR, and solidity, among others. Previous studies have found that incorrect inlet length selection affects turbine performance due to velocity magnitude errors at the turbine [16, 17]. To effectively validate the numerical results, the total depth and width of the computational domain matched the experimental dimensions in [14] setting a length of $2\,d_T$ and $5.5\,d_T$, respectively. A similar case occurs with the position of the outlet in the computational domain as this boundary should be positioned far enough to allow for flow development and guarantee no interference with wake dynamics. When seeking to characterize both near and far wake dynamics, a long enough computational domain must be implemented. Previous studies on wind turbines [18] and hydrokinetic turbines [19, 20] have used outlet lengths equal or greater than $30\,d_T$ downstream of the turbine and have obtained satisfactory results, even in the near wake region.

B. *Rotating domain*

When dealing with rotating domains, increased accuracy of the flow is obtained by modelling the effect of the rotation of the domain on the flow. Simplified techniques such as the Actuator Disk (AD) [21, 22] and the Multiple Reference Frame technique [23, 24] are commonly used techniques due to the reduction of computational cost. However, in AD the aerodynamic forces must be previously determined from measured airfoil characteristics. Also, this method is not sufficient to correctly simulate the development of the turbine's wake as the far wake is sensitive to the stability of the vortical structures in the near wake, which are not captured by this technique [25]. On the other hand, previous studies using the MRF have underestimated turbine power production and low turbulence intensity values in the wake attributed to the inability of this method to resolve the rotation-induced turbulent intensity, as the domain is placed at a specific position (frozen rotor) [26]. To capture the unsteady effects in turbulent flows with rotating domains, a technique known as Sliding Mesh (SM) is widely used. In contrast to MRF, the SM technique allows the sliding of the mesh relative to other zones along the interfaces between them, increasing the computational resources and simulation time [27]. Multiple studies have implemented this technique to estimate power production and characterize the wake in turbines obtaining good concordance with experimental data [15, 28]. For these reasons, the SM technique has been used in this present study.

C. *Turbulence Model*

The Shear Stress Transport (SST) $k-\omega$ turbulence model developed by Menter [29] has been adopted in this study. Past studies have applied this model to numerically capture the flow field around wind [30] and hydrokinetic turbines [11, 31], obtaining good agreement with experimental data compared to other two-equation turbulence models.

D. *Boundary conditions*

A constant, uniform velocity and turbulence were set at the inlet of the domain. These values matched experimental hub-height average values in [14] of U_{in} = 1.04 m/s for velocity in the axial (flow) direction and I_{in} = 5% for the turbulent intensity. The outlet of the domain was set to a gauge uniform pressure of P_{out} = 0 Pa and a turbulent intensity of I_{out} = 5%. For the surface of the domain, a symmetry boundary condition was set. Finally, for the side and bottom faces of the channel as well as the rotor, nacelle and supporting tower's walls, a no-slip condition was used. All boundary conditions, domains and sizes are visualized in Fig. 1.

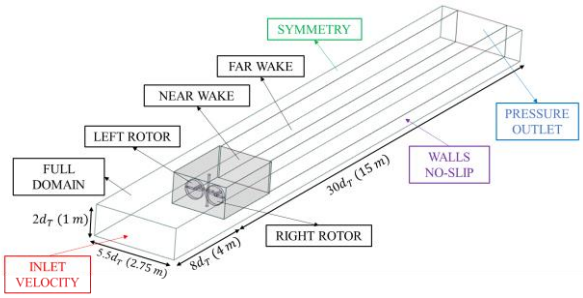

Fig. 1 Computational domain showing employed boundary conditions, subdomains and sizes.

E. *Mesh and time-step*

The computational domain consists of five subdomains that facilitated the creation and refinement of the mesh while also the rotation specification. All subdomains are visualized in Fig. 1. Each of the turbine's rotors is embedded in a rotating subdomain with a diameter 10% larger than d_T, separated and connected to the stationary subdomain by a sliding mesh. Similar meshes were guaranteed to be in both faces creating the interface necessary for the sliding mesh, assuring accuracy and stability while performing the transient analysis. A well-refined mesh was created in the vicinity of the walls in order to capture and achieve an accurate solution of the boundary layer. A y^+ = 1 value was ensured across the rotors, nacelles, supporting arms, and tower. Additional refinements were conducted on the near, far, and full domains with the aim of tracking the tip vortices. Three different polyhedral meshes were created and labeled as coarse, medium, and fine. The objective variable to perform the grid convergence study was the power coefficient (C_p) averaged over four revolutions. This variable was monitored for a TSR of λ = 5.07 matching experimental condition in [14]. The respective number of cells for each mesh and the averaged C_p values are presented in Table I.

The difference in Cp between the medium and fine grids is well below 2%, and the medium mesh only exhibited a 3% difference compared to experimental data; As a compromise between accuracy and computation time, the medium grid was selected for this study.

TABLE I
AVERAGED C_p FOR THE THREE EMPLOYED GRIDS AND EXPERIMENTAL VALUE

Mesh	Cells [Millions]	Averaged C_p [-]
Coarse	19.89	0.430
Medium	21.93	0.461
Fine	48.01	0.468
Experimental	--	0.476

The time-step preliminary analysis considered three different cases: Δt = 0.00001, 0.0001 and 0.0003 s. Using a time-step of Δt = 0.0003 s yielded a 3% difference with experimental data in [14] and a difference below 1% compared to a time-step of Δt = 0.00001. For this reason, a Δt = 0.0003 s was selected for all simulations as computation time was significantly reduced.

III. RESULTS & DISCUSSION

F. *TSR versus C_p*

For validation purposes and to show the advantage that the SST $k-\omega$ turbulence model has when dealing with different type of flows, three TSRs (λ = 3, 5.07 and 7.6) were simulated and compared to experimental data in [14]. All averaged C_p values are presented in Table II.

TABLE II
COMPARISON OF AVERAGED NUMERICAL AND EXPERIMENTAL [14] C_p FOR THREE TSR (λ) STUDIED

TSR (λ)	Experimental C_p [-]	Averaged C_p [-]
3	0.320	0.310
5.07	0.476	0.461
7.6	0.368	0.382

Comparing numerical results to experimentally recorded values in [14], a difference of 3% for the lowest TSR studied (λ = 3) and a 4% for the highest TSR (λ = 7.6), were obtained. In both values of TSR, stall is expected to happen, causing an adverse pressure gradient and hence, power production decreases. All numerical results are in an acceptable range with experimental data, highlighting the advantage and ability of the SST $k-\omega$ turbulence model in dealing with a variety of flows.

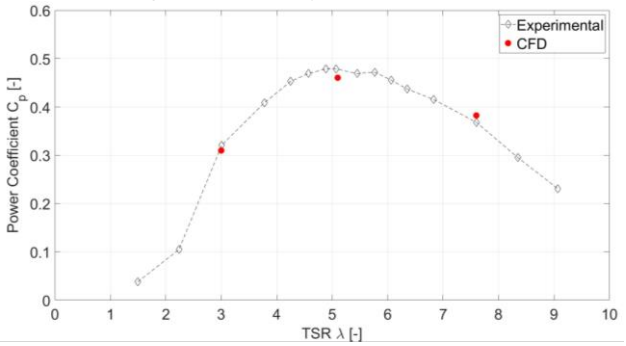

Fig. 2 C_p comparison obtained in the present numerical study versus experimental in [14].

Fig. 2 presents three simulated numerical values for C_p over a range of TSR obtained experimentally in [14]. It is apparent that the torque, which finally creates the power production, changes as a function of TSR, causing a highly variable and fluctuating power production.

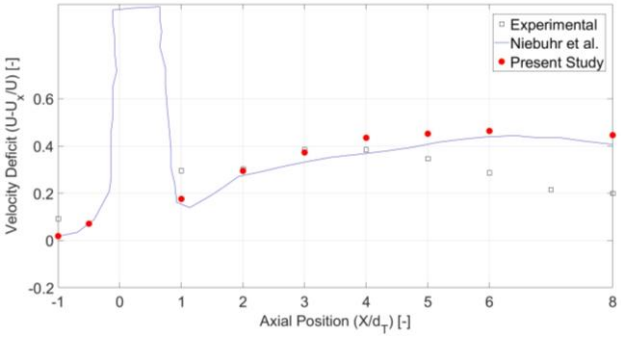

Fig. 3 Velocity deficit at hub height and center of the channel obtained in the present numerical study versus experimental data in [14] and the CFD numerical simulation in [15].

The velocity deficit is a commonly used variable to represent the velocity recovery in the wake of this type of devices. Fig. 3 shows the velocity deficit profile at hub height and center of the channel obtained experimentally in [14] and by the present numerical simulations performed from distances from X/d_T = -1 up to X/d_T = 8. Although the results obtained by the SST $k-\omega$ had good agreement with experimental results for the C_p, the same agreement was not achieved for characterizing the full wake. Comparable results were found by similar numerical simulations performed using the same turbulence model in [15], where authors found the inadequate capture of the wake dissipation rate using different RANS models.

Fig. 3 indicates an appreciable difference in the velocity deficit at X/d_T = 1 and for further distances than X/d_T > 5. However, a difference less than 5% was found between the region of $2 \leq X/d_T \geq 4$. Although the results did not completely capture the wake dynamics in magnitude correctly, the trend of the velocity deficit is similar to the experimental data.

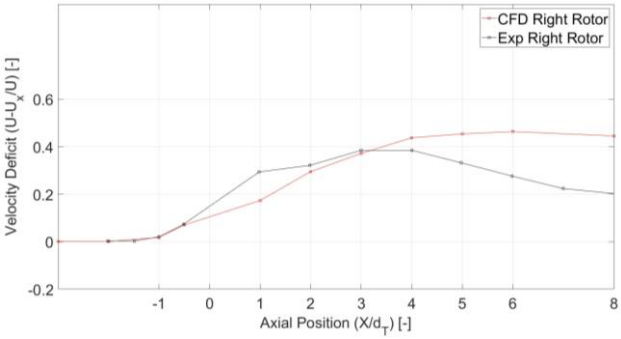

Fig. 4 Velocity deficit at hub height and right rotor's center (Y/d_T = 0.7) obtained in the present numerical study versus experimental data in [14].

Fig. 4 shows the velocity deficit for the right rotor at hub height. Due to the uncertainties of the experimental performance results, especially on the left rotor, only results for the right rotor are presented. Numerical results predict well the beginning of the deceleration of the flow around $X/d_T \approx 1.5$, as the velocity deficit begins to increase, which was also reported in [14]. However, Hill et al. reported a velocity deficit peak of approximately 0.3 at $X/d_T \approx 3$, which was not the case for the numerical

simulations, reaching a peak of 0.46 close to X/d_T = 6, for the right rotor. After the peak in the velocity deficit, the fluid mixes with the bypass flow and begins to gradually recover as the velocity deficit begins to decrease.

Higher velocity deficits compared to experimental data can be attributed to multiple reasons such as the inappropriate estimation of the dissipation rate by URANS models like the SST $k-\omega$, as previously found in studies like [15], the assumption on dealing with isotropic turbulence imposed by the Boussinesq approximation in RANS models and the lack of resolving small eddies. Also, it is key to highlight that the mesh used for studying the wake was chosen by the independency study presented in section E, where the C_p was selected as the parameter for convergence and possibly ignoring the effect that the spatial discretization of the regions behind the rotor might have on the wake representation.

G. *Influence of rotor spacing*

A considerable portion of a tidal channel cross-section must be unblocked to allow for navigation of vessels and so forth, limiting the space covered by turbines placed across the channel's width. Due to this limitation, it is key to find the optimal spacing between the turbines that maximizes power production while minimizing the width occupied by the devices. In this study, three different lateral spacings (L/d_T) were studied corresponding to L/d_T = 1.2, 1.4 and 1.6, where L is the axial distance between both the rotor's center.

TABLE III
AVERAGED C_p FOR THREE LATERAL SPACINGS (L/d_T) STUDIED

Lateral Spacing (L/d_T) [-]	Averaged C_p [-]
1.2	0.449
1.4	0.461
1.6	0.478

Table III presents the C_p for all three lateral spacing cases studied, showing a tendency of a higher C_p as the two rotors are farther spaced out. Increasing the lateral spacing from L/d_T = 1.2 to 1.4 and from 1.4 to 1.6 generated an increase of 2.6% and 3.7% on the C_p, respectively. This behavior can be explained by the choking effect, i.e., reduced flow through the swept area of both rotors. However, this 3.7% increase on the C_p is obtained by establishing a greater separation between the rotors which, from a structural point of view, translates into an increase in the bending and torsional moments that the central structure must support. For this reason, the central tower will probably have to be designed using materials with higher mechanical properties or with a larger diameter/thickness, increasing manufacturing and implementation prices of these devices. This price increase will in turn increase the project's levelized cost of energy (LCOE) and should be carefully analyzed to see if the increased rotor spacing ultimately has a positive economic impact.

IV. CONCLUSIONS

A 1:40 scale model of the US DOE RM1, an axial-flow dual counter-rotating rotors tidal turbine was numerically studied by means of CFD. Three-dimensional simulations using SM technique and SST $k-\omega$ turbulence model, have been implemented to estimate C_p in a range of TSR. Numerical results showed a favorable comparison with experimental data, exhibiting a difference lower than 4% for all TSR studied.

Although good agreement with experimental results for the C_p was achieved, the same agreement was not accomplished for characterizing the wake. Numerical results estimated higher velocity deficits at distances $X/d_T > 3$, hence estimating a delayed wake recovery. This behavior was attributed to multiple factors such as an incorrect estimation of the dissipation rate by URANS models, the assumption on dealing with isotropic turbulence, and the lack of resolving small eddies.

Further, the relationship between rotor spacing and power extraction was studied by numerically simulating three lateral spacings corresponding to L/d_T = 1.2, 1.4 and 1.6. Results showed a tendency of a higher C_p as the two rotors are farther spaced out. An increase from L/d_T = 1.4 to 1.6 caused an increment of 3.7% on C_p. However, this increment is also related to higher torsional and bending moments on the central tower as the rotors are spaced wider apart. A detailed structural and economic study should be performed in order to determine if this increase on the C_p will ultimately cause more competitive LCOE.

V. REFERENCES

[1] REN21, "Renewables 2022 Global Status Report," Paris, 2022.

[2] IEA, "Renewables 2021 Anaysis and forecasts to 2026," 2021.

[3] A. Qaza, F. Hussain, N. A. Rahim, G. Hardaker, D. Alghazzawi, K. Shaban and K. Haruna, "Towards Sustainable Energy: A Systematic Review of Renewable Energy Sources, Technologies, and Public Opinions," *IEEE Access,* vol. 7, pp. 63837-63851, 2019.

[4] J. V. Hernandez Fontes, L. M. Martinez, A. Wojtarowski, J. L. Gonzalez Mendoza, R. Landgrave and R. Silva, "Is ocean energy an alternative in developing regions? A case study in Michoacan, Mexico," *Journal of Cleaner Production,* vol. 266, 2020.

[5] L. Kilcher, M. Fogarty and M. Lawson, "Marine Energy in the United States: An Overview of Opportunities," National Renewable Energy, Golden, 2021.

[6] A. Hoseyni-Chime and P. C. Malte, "HYDROKINETIC TURBINES AT HIGH BLOCKAGE RATIO," in *Marine Energy Technology Symposium*, Seattle, 2014.

[7] C. A. Consul, R. H. J. Willden and S. C. McIntosh, "Blockage effects on the hydrodynamic performance of a marine cross-flow turbine," *Philosophical Transactions of the Royal Society A,* vol. 371, pp. 1-16, 2013.

[8] T. Kinsey and G. Dumas, "Impact of channel blockage on the performance of axial and," *Renewable Energy,* vol. 103, pp. 239-254, 2017.

[9] O. Pacot, D. Pettinaroli, J. Decaix and C. Munch-Alligne, "Cost-effective CFD simulation to predict the performance of a

hydrokinetic turbine farm," in *IOP Conference Series: Earth and Environmental Science*, 2019.

[10] H. W. Ren, F. A. Z. M. Saat, F. S. Anuar, M. A. A. Wahap, E. M. Tokit and T. B. Tuan, "Computational Fluid Dynamics Study of Wake Recovery for Flow Across Hydrokinetic Turbine at Different Depth of Water," *CFD Letters,* vol. 13, no. 2, pp. 62-76, 2021.

[11] A. Benavides-Moran, L. Rodriguez-Jaime and S. Lain, "Numerical Investigation of the Performance, Hydrodynamics, and Free-Surface Effects in Unsteady Flow of a Horizontal Axis Hydrokinetic Turbines," *Processes,* vol. 10, p. 69, 2021.

[12] T. Javaherchi, N. Stelzenmuller, J. Seydel and A. Aliseda, "Experimental and Numerical Analysis of a Scale-model Horizontal Axis Hydrokinetic Turbine," in *2nd Marine Energy Technology Symposium*, Seattle, 2014.

[13] T. Javaherchi, N. Stelzenmuller and A. Aliseda, "Experimental and numerical analysis of the performance and wake of a scale-model horizontal axis marine hydrokinetic turbine," *JOURNAL OF RENEWABLE AND SUSTAINABLE ENERGY,* vol. 9, 2017.

[14] C. Hill, V. S. Neary, M. Guala and F. Sotiropoulos, "Performance andWake Characterization of a Model Hydrokinetic Turbine: The Reference Model 1 (RM1) Dual Rotor Tidal Energy Converter," *Energies,* vol. 13, no. 19, p. 5145, 2020.

[15] C. M. Niebuhr, S. Schmidt, M. van Dijk, L. Smith and V. S. Neary, "A review of commercial numerical modelling approaches for axial hydrokinetic turbine wake analysis in channel flow," *Renewable and Sustainable Energy Reviews,* vol. 158, 2022.

[16] A. Rezaeiha, I. Kalkman and B. Blocken, "Towards accurate CFD simulations of vertical axis wind turbines at different tip speed ratios and solidities: Guidelines for azimuthal increment, domain size and convergence," *Energy Conversion and Management,* vol. 156, pp. 301-316, 2018.

[17] A. Rezaeiha, I. Kalkman and B. Blocken, "CFD simulation of a vertical axis wind turbine operating at a moderate tip speed ratio: Guidelines for minimum domain size and azimuthal increment," *Renewable Energy,* vol. 107, pp. 373-385, 2017.

[18] H. D. Nedjari, O. Guerri and M. Saighi, "CFD wind turbines wake assessment in complex topography," *Energy Conversion and Management,* vol. 138, pp. 224-236, 2017.

[19] M. E. Harrison, W. M. J. Batten, L. E. Myers and A. S. Bahaj, "Comparison between CFD simulations and experiments for predicting the far wake of horizontal axis tidal turbines," *IET Renewable Power Generation,* vol. 4, no. 6, pp. 613-627, 2010.

[20] V. Neary, B. Gunawan, C. Hill and L. P. Chamorro, "Near and far field flow disturbances induced by model hydrokinetic turbine: ADV and ADP comparison," *Renewable Energy,* vol. 60, pp. 1-6, 2013.

[21] G. N. Barakos, T. Fitzgibbon, A. N. KUSYUMOV, S. A. KUSYUMOV and S. A. MIKHAILOV, "CFD simulation of helicopter rotor flow based on unsteady actuator disk model," *Chinese Journal of Aeronautics,* vol. 33, no. 9, pp. 2313-2328, 2020.

[22] C. E. Badoe, M. Edmunds, A. J. Williams, A. Nambiar, B. Sellar, A. Kiprakis and I. Masters, "Robust validation of a generalised actuator disk CFD model for tidal turbine analysis using the FloWave ocean energy research facility," *Renewable Energy,* vol. 190, pp. 232-250, 2022.

[23] L. Menegozzo, A. Dal Monte, E. Benini and A. Benato, "Small wind turbines: A numerical study for aerodynamic performance assessment under gust conditions," *Renewable Energy,* vol. 121, pp. 123-132, 2018.

[24] R. Franzke, S. Sebben, T. Bark, E. Willeson and A. Broniewicz, "Evaluation of the Multiple Reference FrameApproach for the Modelling of an Axial Cooling Fan," *Energies,* vol. 12, no. 15, p. 2934, 2019.

[25] S. Kang, X. Yang and F. Sotiropoulos, "On the onset of wake meandering for an axial flow turbine in a turbulent open channel flow," *Journal of Fluid Mechanics,* vol. 744, pp. 376-403, 2014.

[26] J. Liu, H. Lin and S. R. Purimitla, "Wake field studies of tidal current turbines with different numerical methods," *Ocean Engineering,* vol. 117, pp. 383-397, 2016.

[27] C. Yang and Z. S. Mao, "Multiphase stirred reactors," in *Numerical Simulation of Multiphase Reactors with Continuous Liquid Phase*, London, Elsevier, 2014, pp. 75-151.

[28] O. D. Lopez Mejia, O. E. Mejia, K. M. Escorcia, F. Suarez and S. Lain, "Comparison of Sliding and Overset Mesh Techniques in the Simulation of a Vertical Axis Turbines for Hydrokinetic Applications," *Processes,* vol. 9, p. 1933, 2021.

[29] F. R. Menter, "Two-Equation Eddy-Viscosity Turbulence Models for Enfineering Applications," *American Institute of Aeronautics and Astronautics,* vol. 32, no. 8, pp. 1598-1605, 1994.

[30] S. Yadav, S. V. Veeravalli and S. N. Singh, "COMPARISON OF PREDICTED PERFORMANCE OF VERTICAL AXIS WIND TURBINE USING OVERSET MESH AND SLIDING MESH," in *International Conference on Applied Energy*, Västerås, 2019.

[31] N. Tonello, Y. Eude, B. de Laage de Meux and M. Ferrand, "Frozen Rotor and Sliding Mesh Models Applied to the 3D Simulation of the Francis-99 Tokke Turbine with Code_Saturne," in *Journal of Physics: Conference Series*, Lulea, 2017.